The sensitivity of modeled ozone to the temporal distribution of point, area, and mobile source emissions in the eastern United States

Patricia Castellanos[†], Sheryl H. Ehrman[†], Jeffrey W. Stehr[‡], Russell R. Dickerson[‡],*

Department of Chemical and Biomolecular Engineering, and Department of Atmospheric and Oceanic Science, University of Maryland, College Park, MD 20742

patti@umd.edu, sehrman@umd.edu, stehr@atmos.umd.edu, russ@atmos.umd.edu

Submitted December 12, 2008.

*Corresponding author phone: 301 405 1917; e-mail: sehrman@umd.edu; present address: Department of Chemical and Biomolecular Engineering, 2113 Bldg 90, University of Maryland, College Park, MD 20742.

[†]Department of Chemical and Biomolecular Engineering.

[‡]Department of Atmospheric and Oceanic Science

Abstract

Ozone remains one of the most recalcitrant air pollution problems in the US. Hourly emissions fields used in air quality models (AQMs) generally show less temporal variability than corresponding measurements. In order to understand how the daily cycle of estimated emissions affects modeled ozone, we analyzed the effects of altering all anthropogenic emissions' temporal distributions by source group

1

on 2002 summer-long simulations of ozone using the Community Multi-Scale Air Quality Model (CMAQ) v4.5 and the carbon bond IV (CBIV) chemical mechanism with a 12 km grid. We find that when mobile source emissions were made constant over the course of a day, 8-hour maximum ozone predictions changed by ±7 parts per billion by volume (ppbv) in urban areas on days when ozone concentrations greater than 80 ppbv were simulated in the base case. Increasing the temporal variation of point sources resulted in ozone changes of +6 and –6 ppbv, but only for small areas near sources. Changing the daily cycle of mobile source emissions produces substantial changes in simulated ozone, especially in urban areas at night; implications for abatement strategy are discussed.

Brief

Nine simulations are conducted with an air quality model in order to analyze the sensitivity of modeled ozone to the temporal distribution of emissions source groups.

1. Introduction

Ozone concentrations exceeding the 0.08 parts per million by volume (ppmv) 8-hour average National Ambient Air Quality Standard (NAAQS) are a longstanding problem in many Northeast urban/suburban areas (*1*). Ozone forms in a photochemical mechanism involving nitrogen oxides (NO_x) and volatile organic compounds (VOCs) that is driven by high temperatures and sunlight (*2*). Now that the 75 parts per billion by volume (ppbv) 8-hour average standard has been put forth, there is additional pressure on policy makers to create effective emissions control strategies of these precursor species on a local and regional level. Because overall emissions have decreased significantly following the NO_x SIP call and the introduction of lower emitting vehicles to the fleet, many regulators are focusing on reducing emissions at peak ozone forming hours. For example, in 2007 the states of the Ozone Transport Commission (OTC) signed a memorandum of understanding to reduce emissions from peaking units on high electrical demand days (HEDD). These units are otherwise largely unregulated, often the dirtiest units in the region, and operate on the hottest days of the year.

Air quality models (AQMs) that simulate chemistry, transport, and atmospheric removal processes of multiple pollutants including trace gases and aerosols, are an important tool for studying ozone. They have been used for decision support, regulatory attainment analysis, creation of emissions control strategies and experiments in atmospheric chemistry and transport (*3*). Although in many instances AQMs satisfactorily replicate ozone when compared to surface observations (*4-8*), the simulations are subject to uncertainty (*9*) resulting from parameterizations and approximations embedded in the model algorithms and chemical mechanisms, as well as inaccuracies in the meteorological and emissions inputs (*9-12*). Emissions inventories, reported as annual or daily average values, must be broken up into the hourly fluxes required by AQMs using generalized temporal distributions. Emissions estimates used in the model are less variable than corresponding measurements from continuous emissions monitors (CEM) and field campaigns would imply (*11-13*). Peaking units, for instance, are not currently represented in the model. We would like to know what affect the temporal variability of emissions has on ozone in the model in order to understand the results of implementing detailed emissions control strategies that target time of day.

In a previous study, Tao et al. (2004) compared a uniform simulation in which anthropogenic emissions did not vary from hour-to-hour to a time-varying simulation in which the emissions varied according to temporal profiles included in National Emissions Inventory (NEI) estimates. Their goal was to determine if the effect of misrepresentation of temporal distributions was large enough to warrant the added expense of obtaining better distributions. They found that, when uniform temporal profiles are used on a regional scale (with 90 km resolution), the change in the weeklong average hourly ozone concentration from the time-varying case over the U.S. was very small during the day. Regression and frequency distribution analysis showed that the two simulations agreed well for higher ozone concentrations but not for lower ozone concentrations. While altering all anthropogenic emissions is warranted for analyzing the overall usefulness of an inventory, this does not result in information that is helpful for developing emissions control strategies because rarely are controls applied to every category of emissions. Instead

regulators begin by analyzing source categories that have similar properties and then work down to specific industries or polluting processes.

In this work we will continue to analyze the sensitivity in the model to altering temporal distributions of emissions. However this study will focus on the Eastern U.S. and implement a smaller grid size in order to capture urban effects. We will look at the temporal sensitivities individually of the four major source categories of anthropogenic emissions (area, point, on-road mobile, and non-road mobile sources) as a cursory look at the sensitivity in the model to similar emissions sources.

2. Methodology
Modeling Domain. In this work, a 12 km grid covering the eastern half of the U.S. was used. It was nested within a 36 km grid that covered the continental U.S. and provided the boundary conditions for the finer grid. The 36 km simulation was conducted only once, with boundary conditions provided by a global simulation with the GEOS-CHEM model. Thus each 12 km simulation had the same boundary conditions. A Lambert Conformal grid projection centered at 40N and 97W with the lower left corner located at 264 km west and 888 km south of the center defined the 12 km grid, which contained 172 x172 grid cells. A terrain following σ coordinate defined 22 layers from the surface to roughly 30 km. The first twelve layers fell within the bottom 1.5 km of the atmosphere.

Emissions. We modeled three daily temporal profiles of emissions from area, point, on-road mobile, and non-road mobile sources: a "uniform" temporal profile in which the emissions were the same from hour to hour, a "base" temporal profile, which utilized the temporal distribution provided in the inventories, and an "increased variability" temporal profile in which 50% of nighttime emissions were added to the daytime in order to increase the relative peak during the day and the magnitude of the daily fluctuation in emissions. The uniform and increased variability scenarios were chosen to test the limits of the models sensitivity, and are not meant to represent realistic control strategies. Biogenic emissions were not altered because known sensitivities to temperature, radiation, and relative humidity drive the diurnal variation. In total, nine simulations were conducted with different combinations of emissions

temporal profiles listed in Table 1. The emissions in each grid cell at any hour may be different in each simulation, but the total emissions integrated over the length of the simulation remained the same.

Run Name	Run Code	Area Temporal Profile	Point Temporal Profile	Non-road Temporal Profile	Mobile Temporal Profile
Base Case	BC	Base	Base	Base	Base
Area Uniform	AU	Uniform	Base	Base	Base
Point Uniform	PU	Base	Uniform	Base	Base
Non-road Uniform	NU	Base	Base	Uniform	Base
Mobile Uniform	MU	Base	Base	Base	Uniform
Area Increased Variability	AI	Increased Variability	Base	Base	Base
Point Increased Variability	PI	Base	Increased Variability	Base	Base
Non-road Increased Variability	NI	Base	Base	Increased Variability	Base
Mobile Increased Variability	MI	Base	Base	Base	Increased Variability

Table 1. List of simulations and emissions combinations.

A 2002 emissions inventory (EI) provided by the following four regional planning organizations was processed with the Sparse Matrix Operator Kernel Emissions (SMOKE) v2.2 processor (*15*): the Mid-Atlantic/Northeast Visibility Union (MANE-VU), the Mid-West Regional Planning Organization (MRPO), the Visibility Improvement State and Tribal Association of the Southeast (VISTAS), and the Central Regional Air Planning Association (CENRAP). The 2002 EI was developed to support the 8-hour ozone NAAQS attainment demonstration State Implementation Plans (SIP) in the eastern U.S. Details of the inventory and emissions processing can be found in NYSDEC (2006a, 2007) and Pechan (2006).

Meteorology. The meteorological fields were generated for the domain with the Penn State/NCAR 5th Generation Mesoscale Model 5 (MM5) v3.6 (*19*) by the University of Maryland in support of the 8-hour

ozone SIPs. Details and analysis of the simulation can be found in NYSDEC (2006b), and a brief description of the simulation details is given in Supporting Information I.

Air Quality Model. The emissions and meteorology were used as inputs into the Community Multiscale Air Quality Model (CMAQ) v4.5 (*21*). CMAQ is a three-dimensional Eulerian grid model that simulates atmospheric chemistry, aerosol formation and dynamics, transport of pollutants, and pollutant removal processes. In this implementation, the carbon bond IV (CBIV) gas-phase chemical mechanism (*22*) and the AE3/ISOROPPIA aerosol reaction scheme were used along with the Euler backward iterative (EBI) solver. Daily photolysis rate constant lookup tables were generated with the JPROC software included in CMAQ. The Piecewise Parabolic Method was used as the horizontal advection algorithm. The simulation began on May 1st with clean initial conditions and ended on September 15. The seasonal simulation allows us to evaluate the model over different time scales and meteorological conditions (*23*). The first 15 days were taken as spin up, and not used in the analysis.

Observational Data & Model Performance Evaluation. A model performance evaluation was carried out on the base case simulation during the 8-hour NAAQS attainment demonstration SIP using a comprehensive set of measurements at the surface and aloft. Details of the assessment and a list of the various national and regional measurement networks can be found in NYSDEC (2006c). Simulated concentrations of the following species in Virginia and the Ozone Transport Region (OTR) (comprised of Connecticut, Delaware, Maine, Maryland, Massachusetts, New Hampshire, New Jersey, New York, Pennsylvania, Rhode Island, Vermont, Northern Virginia, and the District of Columbia) were analyzed: ozone, particulate matter less than 2.5 μm (PM2.5), CO, NO_x, SO_2, and non-methane hydrocarbons, as well as wet deposition rates of SO_4^{2-}, NH_4^+, and NO_3^-. The threshold statistics listed in Table S1 (Supporting Information) suggested by EPA (*25*) for model performance evaluation were calculated for ozone when model and measurement data were paired in time and space (without interpolation). The data from July 6-9 were excluded because long-range transport of pollutants from forest fires taking place in Quebec was not accounted for in the model. A summary of the results from this study and the

model performance evaluation conducted by Eder et al. (2006) for the continental U.S. can be found in Supporting Information II.

3. Results

Emissions. Typical day (August 21, 2002) domain total hourly NO_x emissions are shown in Figure 1 for the nine simulations. In Figure 1(a), changing the diurnal variation of mobile sources to uniform has the greatest change on the domain total NO_x diurnal variation. The MU case has an up to 50% increase in emissions at night, and a 10-20% decrease in emissions during the day, while the AU, PU, and NU cases increase nighttime NO_x emissions by up to 10% and decrease daytime NO_x emissions by up to 4%. This is expected because mobile source emissions contain the most temporal variability in the NO_x base case inventory (Figure 2). In Figure 1(b), increasing the temporal variation of point sources has the greatest change from the base case because point sources make up the largest fraction of the NO_x base case inventory at night (Figure 2). The PI case has an up to 25% decrease in emissions at night, and an up to 13% increase in emissions during the day, while in the other three increased variability simulations' NO_x emissions decrease by up to 8% at night and increase by up to 6% during the day. There is very little change in the domain total VOC emissions' diurnal variation when the temporal variation of the four emissions sectors are altered because biogenic emissions, which were not altered, make up 74% and 84% of the total base case VOC emissions inventory during the nighttime and daytime, respectively (Figure 2).
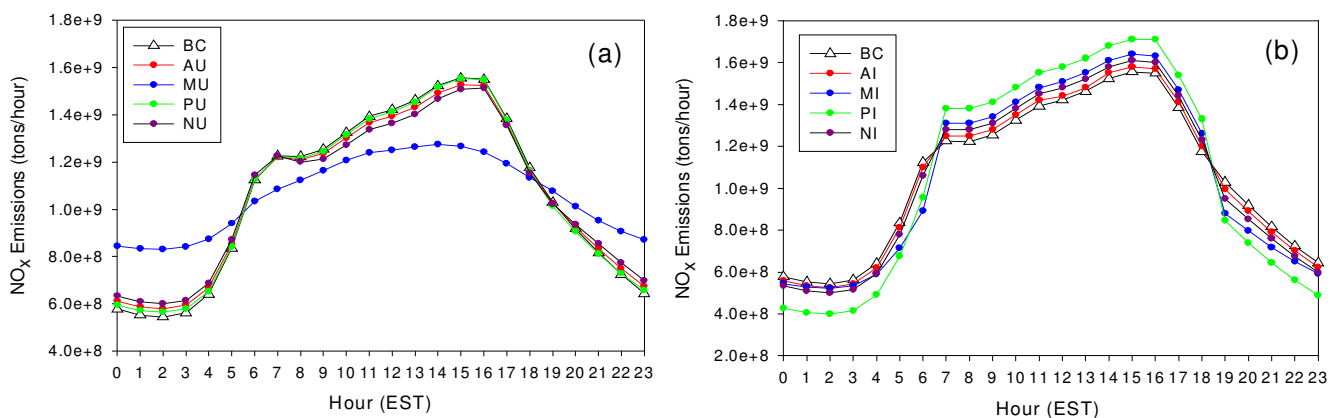

Figure 1. The August 21, 2002 domain total hourly NO_x emissions for the (a) Base Case (BC), Area Uniform (AU), Mobile Uniform (MU), Point Uniform (PU), and Non-road Uniform (NU) simulations,

and the (b) Base Case (BC), Area Increased Variability (AI), Mobile Increased Variability (MI), Point Increased Variability (PI), and Non-road Increased Variability (NI) sensitivity simulations.
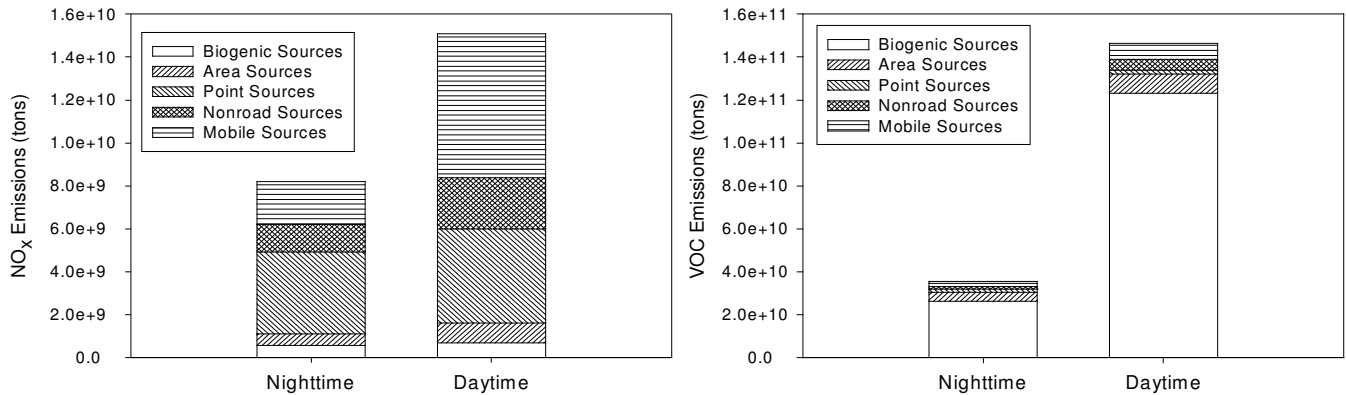

Figure 2. The base case domain total nighttime (12:00 am - 7:00 am EST and 7:00 pm - 12:00 pm EST) and daytime (7:00 am – 7:00 pm EST) NO_x (left) and VOC (right) emissions by emissions sector on August 21, 2002. In the NO_x base case emissions inventory, mobile source emissions contain the most temporal variability, while point source emissions make up the largest fraction of the inventory at night. Because biogenic emissions dominate the VOC emissions inventory, there is very little change in the domain total VOC emissions' diurnal variation when the temporal variations of the four anthropogenic emissions sectors are altered.

Regional Sensitivity to Uniform Temporal Distributions. Deviations from the base case in the daily 8-hour maximum ozone concentration (8HRMAX) by the AU, PU, MU, and NU simulations are taken to be measures of sensitivity in the model predictions to errors in the model inputs, namely the temporal distributions of the emissions sectors, assuming that the base case is a best estimate of emissions. The largest sensitivities averaged over the duration of the simulation occur when the mobile emissions' temporal distributions are made uniform (Figure S1, Supporting Information). The average and standard deviation in time and space of the MU sensitivities were -0.4 ± 0.4 ppbv, while the AU, PU, and NU sensitivities were 0.1 ± 0.1 ppbv, -0.1 ± 0.09 ppbv, and -0.2 ± 0.2 ppbv, respectively. The sensitivities from the area, point, and non-road source categories were much smaller in magnitude and area of

8

influence in comparison to mobile sources, probably because of the small change in emissions. Therefore, the subsequent analysis will focus on the MU simulation.

The sensitivity of the 8HRMAX averaged in time in the MU case was calculated for two subsets of conditions: 1) when an 8HRMAX of 50-80 ppbv occurred, and 2) when greater than 80 ppbv occurred in the base case (Figure 3). The largest sensitivities occur in the latter case. Over land, there is a –7 ppbv (-6%) change in urban/suburban areas, and offshore the sensitivities reach +7 ppbv (+6%) in the North Atlantic. Likewise, in the Northeast industrial corridor and in urban centers in the south, where sensitivities are negative, the number of days (out of the 123 day simulation) where the 8HRMAX exceeds 80 ppbv decreases by 5-8 days from 20-30 days in the base case (Figure S2, Supporting Information).
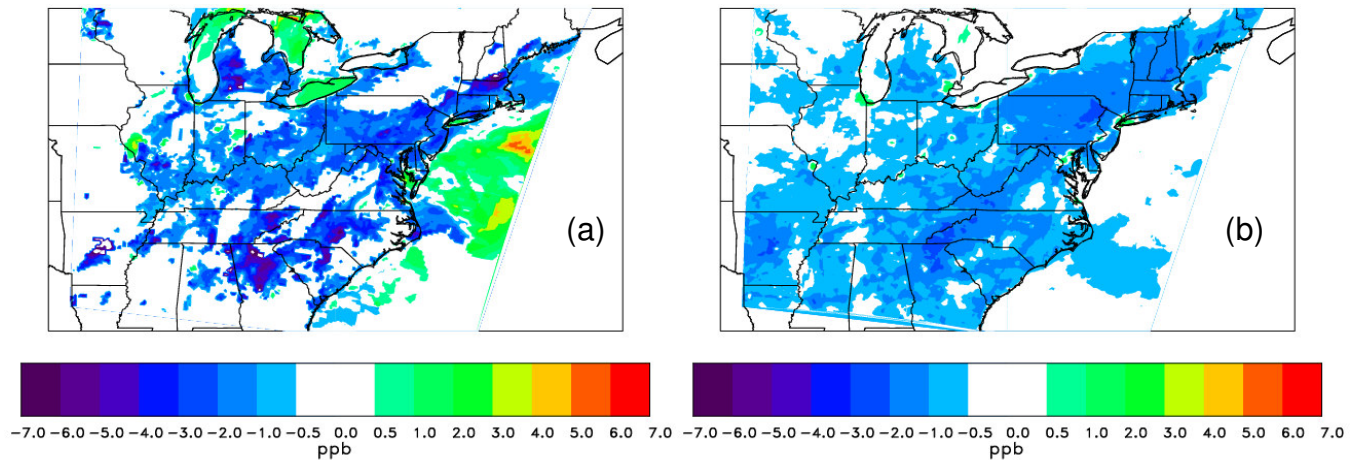

Figure 3. The mean difference between the MU simulation and the base case $\left(\frac{1}{N}\sum Mobile\ uniform - base\ case\right)$ in the daily 8HRMAX in each grid cell from May 15 to September 15 when a) greater than 80 ppbv occurs in the base case, and b) between 50 and 80 ppbv occurs in the base case.

When comparing the frequency distributions of the 8HRMAX in urban and rural areas, we see once again that the greatest sensitivities in the MU case occur in urban areas, close to the source of the emissions, and at high ozone concentrations (Figure S3, Supporting Information). While in rural areas

the frequency distributions for the MU case and the base case remain similar, in urban areas the fraction of 70-95 ppbv 8HRMAX concentrations decrease, and the fraction of 40-60 ppbv 8HRMAX concentrations in the MU simulation increases from the base case, indicating an overall downward shift in urban ozone concentrations.

   Regional Sensitivity to Increased Variation in Temporal Distributions.   When the diurnal variation of each sector of emissions is increased, smaller sensitivities than the uniform cases are observed on average across the board. The increased temporal variability of area and non-road sources has very little effect, corresponding to the small change in emissions. The domain wide average 8HRMAX sensitivities are 0.05 ± 0.07 and 0.06 ± 0.1 ppbv, respectively. The map of sensitivities shows less than 1 ppbv change throughout the domain. Similarly, the 8HRMAX sensitivity of mobile sources averaged in time and space is 0.09 ± 0.2 ppbv. When the base case predictions are binned into the 50 to 80 ppbv and greater than 80 ppbv levels, the average differences between the base case and MI case are 0.08 ± 0.2 ppbv and 0.02 ± 0.5 ppbv, respectively. Consequently, the rural and urban frequency distributions of the 8HRMAX for the MI case do not significantly change from the base case. These small domain wide average sensitivities are slightly misleading, because in some localized areas that are designated as non-attainment areas, and where high ozone occurs in the model there is still an effect (Figure S4, Supporting Information). For example, in the Atlanta area, compared to the base case, up to 5 more exceedances than the base case of the 80 ppbv 8HRMAX level occur as a result of a 2 ppbv increase in ozone, on average (Figure S5, Supporting Information).

   Increasing the temporal variation of point sources also results in small sensitivities averaged in time and space: 0.04 ± 0.3 ppbv (all days), 0.3 ± 0.03 ppbv (when greater than 80 ppbv is predicted), and 0.03 ± 0.4 ppbv (when 50-80 ppbv is predicted). However, larger localized sensitivities in the greater than 80 ppbv bin on the order of +6 ppbv occur near Atlanta, Birmingham, Knoxville, and Nashville (Figure 4). In the Ohio River Valley, small areas of +6 and –6 ppbv sensitivity occur adjacent to each other,

suggesting that, in the model, the effects of changes in emissions from the large point sources located in this region for the most part remain close to the source.
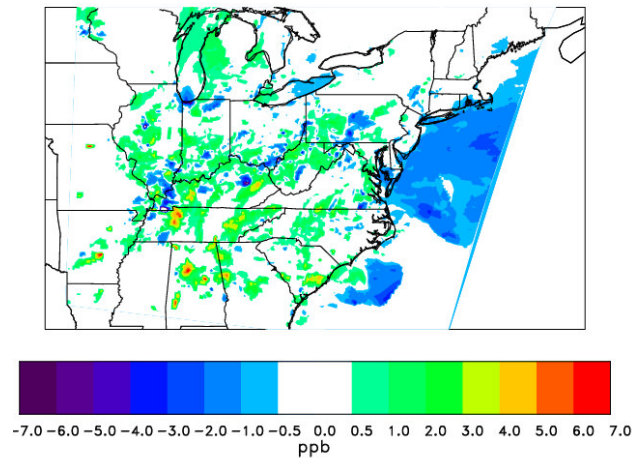

Figure 4. The mean difference between the PI simulation and the base case in the daily 8HRMAX in each grid cell when ozone concentrations greater than 80 ppbv occur in the base case. In the Ohio River Valley, small areas of +6 and –6 ppbv sensitivity occur adjacent to each other, suggesting that, in the model, the effects of changes in emissions from the large point sources remain close to the source.

This result, along with the large sensitivities concentrated in urban areas from the MU simulation, is in agreement with the spatial correlation analysis conducted by Gilliland et al. 2008. They found that when emissions in the model are changed according to measurements before and after the NO_x SIP Call, the subsequent changes in ozone concentrations are a result of changes in emissions sources that are close by rather than transported emissions. In the same study, a comparison of CMAQ to ground observations suggests that CMAQ underestimates the e-folding distance and the effects of transported ozone and emissions from elevated point sources (*26-29*). Therefore, it is likely that the area and magnitude of the sensitivities in the PI and MU simulations are underestimated.

Local Sensitivities. Baltimore in the Northeast and Atlanta in the South were selected for further analysis based on the results of the regional sensitivities. Average hourly ozone measurements at three

monitoring sites near each of the cities were compared to each of the sensitivity simulations: two monitoring sites within the Photochemical Assessment Monitoring Stations (PAMS) network, and one within the Clean Air Status and Trends Network (CASTNET). The CASTNET sites, Arendtsville near Baltimore and Sand Mountain near Atlanta, are located in remote areas and provide data on rural ozone levels. The PAMS monitoring stations are located within and downwind of polluted areas where emissions of precursors and their effects can be observed. Specifically, Essex and Tuckers, the PAMS type 2 sites for Baltimore and Atlanta, respectively, are located within the area of maximum emissions levels. Aldino and Conyers, the PAMS type 3 sites, are situated in a location that is primarily downwind of the maximum emissions from Baltimore and Atlanta, respectively. A map of the locations of the six selected sites is shown in Figure S7, Supporting Information. Site descriptions can be found at http://www.epa.gov/oar/oaqps/pams/ and http://www.epa.gov/castnet/site.html.

Overall, the largest effect on the modeled hourly ozone values at the surface sites in Baltimore and Atlanta occurs at night when mobile emissions are temporally uniform. The increased nighttime emissions from the mobile source group, which are rich in NO_x, in the MU case, build up locally during typically stagnant conditions and cause ozone destruction via NO_x titration. At the Essex and Tucker sites, located within the area of primary emissions, the MU simulation causes hourly ozone values at night to decrease from the base case by up to 10 ppbv. Yet, compared to observations, the MU simulation has better model performance at night than the base case (Figure 5). Conversely, when mobile source temporal variations are increased and NO_x emissions decrease at night, at these sites, the MI simulation nighttime ozone values are slightly higher than the base case.
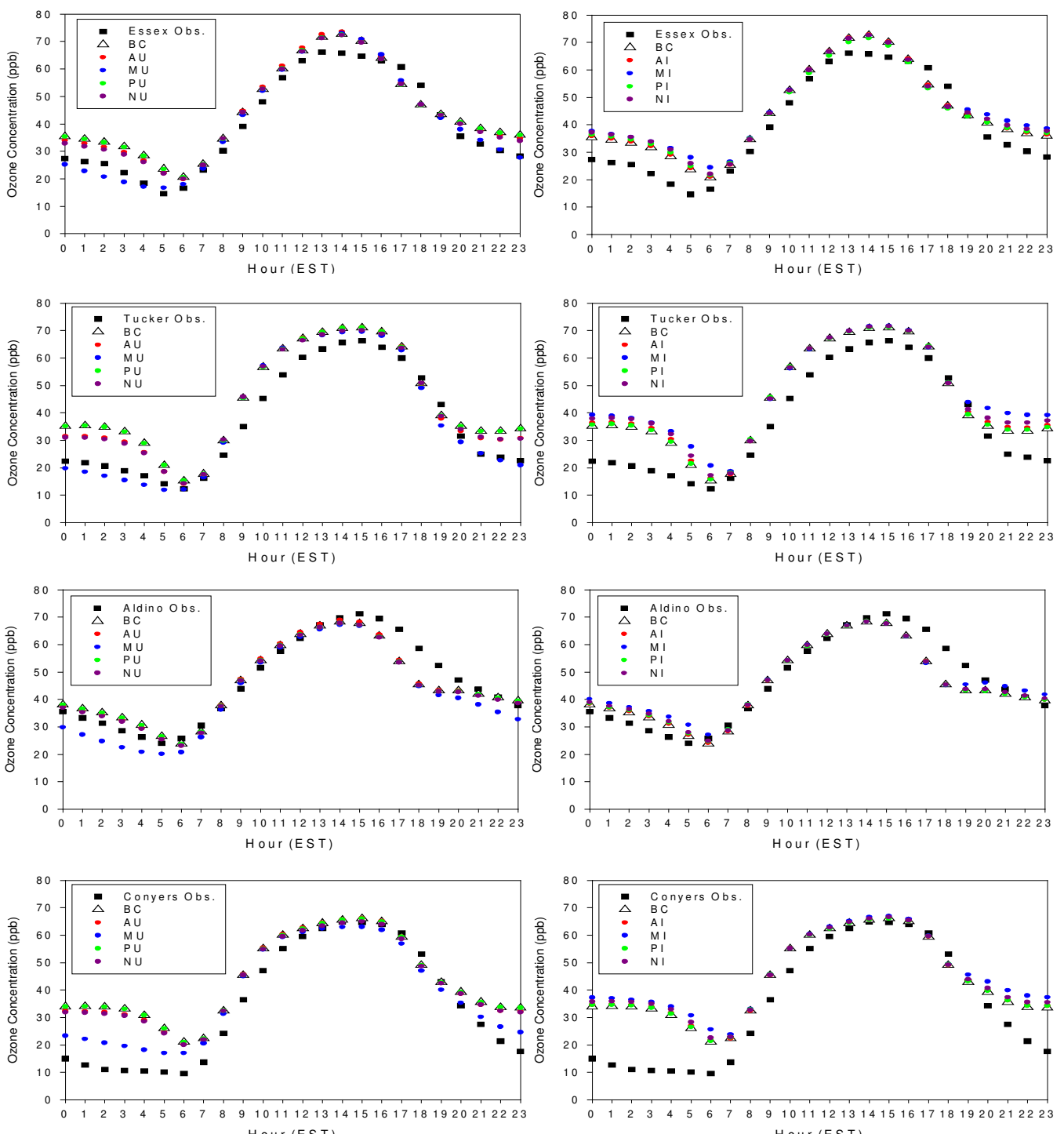
At the Aldino site, downwind of Essex, the nighttime hourly ozone values predicted in the base case are close to measurements. Thus, increasing NO_x emissions at night in the MU simulation results in underestimated ozone at this time. Also, at this site, the model predicts the ozone maximum one hour earlier than the measurements. When the diurnal variation of the emissions is changed in the sensitivity simulations, there is no change in when the peak ozone values occurs (Figure 5). At the Conyers site,

similar to the Tucker site, the model reproduces the diurnal variation of ozone, but overestimates ozone at night. Likewise, the MU simulation lowers the nighttime ozone concentrations from the base case at this site, although ozone predictions remain ~10 ppbv greater than observations (Figure 5).

Capturing the diurnal variation of ozone, especially the nighttime minimum, is dependent on the meteorological model's ability to simulate the diurnal variation of the planetary boundary layer (PBL). Unfortunately, few temporally and spatially detailed boundary layer observation datasets exist that can be used to validate model results. However, Berman et al. (1999) were able to study mixing depths in the Northeast using six rawinsonde stations that conducted soundings every four hours, four radio acoustic sounder system (RASS) sites, and 44 surface stations during the summer of 1995. Rao et al. (2003) evaluated the mixing height from a MM5 simulation of this time period using the Blackadar PBL scheme with the sounding data from the Berman et al. (1999) study and found good agreement at night. Although the Rao et al. (2003) comparison is for a different model year than this study, the acceptable model performance by MM5 of the other observed meteorological variables in this work lends some credence to the assumption that MM5 and the Blackadar PBL scheme do a reasonable job at reproducing nocturnal mixing heights. It follows that the overestimation of nighttime ozone by the base case at the PAMS type 2 sites may be the result of another weakness in the model.

The lower nighttime ozone values at the Essex and Tucker sites in the temporally uniform simulations, especially the MU case, suggest that underestimated NO_x emissions and/or overestimated losses of NO_x at night may also play a role in the nighttime over prediction of ozone by CMAQ in urban areas. This reasoning is appropriate for the Essex site where the NO_x model performance improves in the MU case. The base case underestimates observed nighttime NO_x concentrations by 38%, while the MU case underestimates nighttime NO_x by 10%. However, at the Tucker site, the base case nighttime NO_x concentrations agree well with observations, except for over predictions at the beginning of the evening, while the MU case over predicts nighttime observations by 95%.

At the rural CASTNET sites, Arendtsville and Sand Mountain, the model has a low bias during the day. At night, the model underestimates ozone over Arendtsville, and overestimates ozone over Sand Mountain. Regardless, the sensitivity simulations have very little effect on the model's performance at these rural sites (Figure 5). The low daytime bias may be due to the reaction rate of the hydroxyl radical with NO_2 in CBIV that terminates the hydroxyl radical too quickly during the daytime and inhibits the production of ozone through the oxidation of aldehydes (*32*). This mechanism would be important in rural areas where VOCs from biogenic emissions dominate.
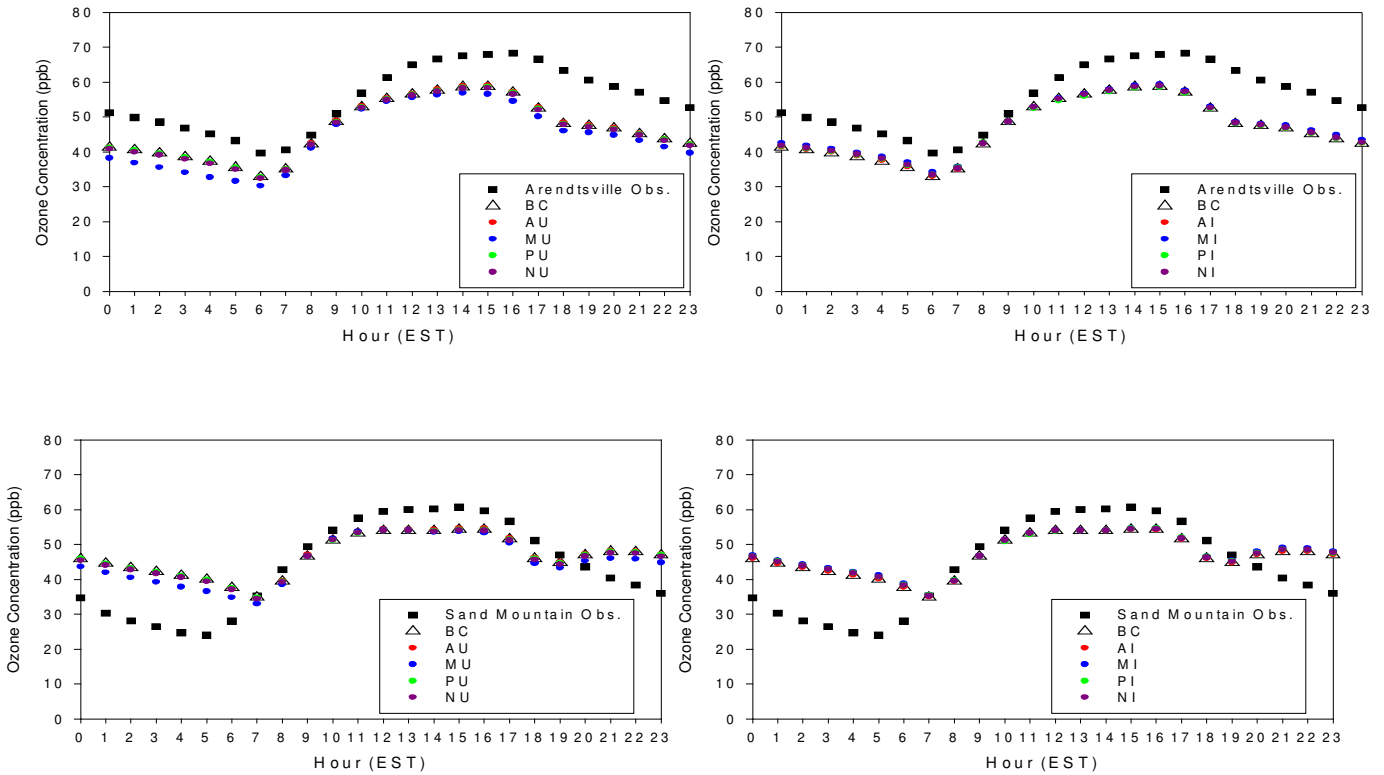
Figure 5. The hourly ozone concentrations averaged in time that were observed (filled boxes) and modeled at the Essex (1st row), Tucker (2nd row), Aldino (3rd row), Conyers (4th row), Arendtsville (5th row) and Sand Mountain (6th row) monitoring sites. The modeled average hourly ozone concentration plots are separated into uniform (left column) and increased variability (right column) groups. The base case (open triangles) is plotted with both groups.

4. Discussion and Implications

In the base case emissions inventory, mobile emissions have the largest temporal variation, and making the temporal variation of this source group uniform caused the largest effects on the 8HRMAX. Particularly, the 8HRMAX decreased in urban areas on days with high (greater than 80 ppbv) ozone by up to 7 ppbv, resulting in a decrease in the number of 80 ppbv exceedances. This result has significant policy implications in terms of calculating relative reductions for demonstrating attainment with the

NAAQS. From a regulatory perspective, the significant decrease in the number of 80 ppbv exceedances in the MU simulations demonstrates that accurate representation of daily variability of mobile emissions is necessary to simulate ozone correctly. The results from this mobile source emissions scenario also demonstrate the upper limits of intentionally shifting traffic patterns as an abatement strategy. If, traffic emissions occurred more at night and less in the day, there would be fewer ozone events. Such a temporal shift might be accomplished by switching to electric cars charged at night, or increasing the number of high occupancy vehicle lanes in a metropolitan region, which would force commuters to drive at off peak hours.

Because point sources are the largest nighttime emitters in the base case emissions inventory, increasing the temporal variation of this source group has the greatest effect. Similar to the result from the MU case, the 8HRMAX and the number of 80 ppbv exceedances increased, but only close to the emissions sources. Near these areas, the 8HRMAX decreases by the same magnitude. This patchy result may be due to the model's weakness at transporting point source emissions, which underestimates the area and magnitude of ozone generated by point source emissions. Because of this weakness and the nature of the temporal variability of the emissions sectors in the base case emissions inventory, the model appears to be able to respond more realistically to emissions control strategies that target the time of day of emissions from mobile sources, than from point, area, or non-road sources.

We find from comparisons at several monitors that the largest differences between the base case and temporal sensitivity simulations occur in the nighttime (similar to Tao et al. (2004)), especially in urban areas when the mobile emissions temporal distribution is uniform. Specifically, model performance is poor at night, but improves in urban areas when mobile emissions are made uniform in time. Correcting model underestimated nighttime NO_x emissions and/or overestimated NO_x losses will enhance the numerical simulation of ozone and our ability to evaluate pollution abatement strategies. Adequate treatment by the model of the night-to-day ozone accumulation process is essential to photochemical modeling (*31*), and will become especially important as emissions and ozone concentrations decrease.

Acknowledgements

Supporting Information Available
Additional figures that show the equations for model performance threshold statistics, and further results from the sensitivity simulations.

Literature Cited
1. U.S. Environmental Protection Agency *The Ozone Report: Measuring Progress through 2003*; 454/K-04-001; Office of Air Quality Planning and Standards, Emissions Monitoring and Analysis Division, U.S. Environmental Protection Agency; Research Triangle Park, NC, April 2004.

2. Seinfeld, J. H.; Pandis, S. N. *Atmospheric chemistry and physics: from air pollution to climate change;* Wiley & Sons: New York, 2006.

3. Russell, A. Regional Photochemical Air Quality Modeling: Model Formulations, History, and State of the Science. *Ann. Rev. Energ. Env.* **1997**, *22*, 537-588.

4. Godowitch, J. M.; Gilliland, A. B.; Draxler, R. R.; Rao, S. T. Modeling assessment of point source NO$_x$ emission reductions on ozone air quality in the eastern United States. *Atmos. Environ.* **2008**, *42* (1), 87-100.

5. Appel, K. W.; Gilliland, A. B.; Sarwar, G.; Gilliam, R. C. Evaluation of the Community Multiscale Air Quality (CMAQ) model version 4.5: Sensitivities impacting model performance Part I-Ozone. *Atmos. Environ.* **2007**, *41*, 9603-9615.

6. Bey, I .J.; D. J.; Yantosca, R. M.; Logan, J. A.; Field, B. D.; Fiore, A. M.; Li, Q. B.; Liu, H. G. Y.; Mickley, L. J.; Schultz, M. G. Global modeling of tropospheric chemistry with assimilated meteorology: Model description and evaluation. *J. Geophys. Res.* **2001**, *106* (D19), 23,073-23,095.

7.   Brunner, D. S., Staehelin, J.; Rogers, H. L.; Kohler, M. O.; Pyle, J. A.; Hauglustaine, D. A.; Jourdain, L.; Berntsen, T. K.; Gauss, M.; Isaksen, I. S. A.; Meijer, E.; van Velthoven, P.; Pitari, G.; Mancini, E.; Grewe, V.; Sausen, R. An evaluation of the performance of chemistry transport models - Part 2: Detailed comparison with two selected campaigns. *Atmos. Chem. Phys.* **2005**, *5*, 107-129.

8.   Eder, B.; Yu, S. A performance evaluation of the 2004 release of Models-3 CMAQ. *Atmos. Environ.* **2006**, *40* (26), 4811-4824.

9.   Fine, J.; Vuilleumier, L.; Reynolds, S.; Roth, P.; Brown, N. Evaluating Uncertainties in Regional Photochemical Air Quality Modeling. *Annu. Rev. Environ. Resour.* **2003**, *28*, 59-106.

10.   Mallet, V.; Sportisse, B. Uncertainty in a chemistry-transport model due to physical parameterizations and numerical approximations: An ensemble approach applied to ozone modeling. *J. Geophys. Res.* **2006**, *111*, D01302.

11.   Placet, M.; Mann, C. O.; Gilbert, R. O.; Niefer, M. J. Emissions of ozone precursors from stationary sources: a critical review. *Atmos. Environ.* **2000**, *34*, 2183-2204.

12.   Hanna, S. R.; Chang, J. C.; Fernau, M. E. Monte Carlo Estimates of Uncertainties in Predictions by a Photochemical Grid Model (UAM-IV) due to Uncertainties in Input Variables. *Atmos. Environ.* **1998**, *32* (21), 3619-3628.

13.   Marr, L. C.; Black, D. R.; Harley, R. A. Formation of photochemical air pollution in central California: 1. Development of a revised motor vehicle emission inventory. *J. Geophys. Res.* **2002**, *107* (D6), 4047.

14.   Tao, Z.; Larson, S. M.; Williams, A.; Caughey, M.; Wuebbles, D. J. Sensitivity of regional ozone concentrations to temporal distribution of emissions. *Atmos. Environ.* **2004**, *38*, 6279-6285.

15.   SMOKE v2.2 User's Manual. http://www.smoke-model.org/version2.2/index.cfm (accessed Dec 2008).

16.   NYSDEC *Processing of Biogenic Emissions for OTC/MANE-VU Modeling;* TSD-1b; New York State Department of Environmental Conservation; Albany, NY 12233, Sep 2006a.

17.   NYSDEC *Emissions Processing for 2002 OTC Regional and Urban 12km Base Year Simulation;* TSD-1c; New York State Department of Environmental Conservation; Albany, NY 12233, March 2007.

18.   Pechan *Technical Support Document for 2002 MANE-VU SIP Modeling Inventories, version 3;* Final Report to the Mid-Atlantic/Northeast Visibility Union; E.H. Pechan & Associates, Inc.: 3622 Lyckan Parkway, Suite 2005, Durham, NC 27707, Nov 2006.

19.   Grell, G. A.; Dudhia, J.; Stauffer, D. R. *A description of the 5th generation Penn State/NCAR Mesoscale Model (MM5)*; NCAR Technical Note 398+STR; National Center for Atmospheric Research: Boulder, CO; 1995.

20.   NYSDEC *Meteorological Modeling using Penn State /NCAR 5th Generation Mesoscale Model (MM5);* New York State Department of Environmental Conservation; Albany, NY 12233, March 2006b.

21.   Byun, D.; Schere, K. L.; Review of the Governing Equations, Computational Algorithms, and Other Components of the Models-3 Community Multiscale Air Quality (CMAQ) Modeling System. *Appl. Mech. Rev.* **2006**, *59*, 51-77.

22.   Gery, M. W.; Whitten, G. Z.; Killus, J. P.; Dodge, M. C. A Photochemical Kinetics Mechanism for Urban and Regional Scale Computer Modeling. *J. Geophys. Res.* **1989**, *94* (D10), 12,925-12,956.

23.   Hogrefe, C.; Rao, S. T.; Zurbenko, I. G.; Porter, P. S. Interpreting the Information in Ozone Observations and Model Predictions Relevant to Regulatory Policies in the Eastern United States. *Bull. Amer. Meteor. Soc.* **2000**, *81* (9), 2083-2106.

24.   NYSDEC *CMAQ Model Performance and Assessment 8-h OTC Ozone Modeling;* New York State Department of Environmental Conservation; Albany, NY 12233, March 2006c.

25.   U.S. Environmental Protection Agency *Compilation of Photochemical Models' Performance Statistic for 11/94 Ozone SIP Applications*, Office of Air Quality Planning and Standards, U.S. Environmental Protection Agency; Research Triangle Park, NC, 1996; p 156.

26.   Gilliland, A. B.; Hogrefe, C.; Pinder, R. W.; Godowitch, J. M.; Foley, K. L.; Rao, S. T. Dynamic evaluation of regional air quality models: Assessing changes in O_3 stemming from changes in emissions and meteorology. *Atmos. Environ.* **2008**, *42*, 5110-5123.

27.   Kim, S. W.; Heckel, A.; McKeen, S. A.; Frost, G. J.; Hsie, E. Y.; Trainer, M. K.; Richter, A.; Burrows, J. P.; Peckham, S. E.; Grell, G. A. Satellite-observed US power plant NO_x emission reductions and their impact on air quality. *Geophys. Res. Lett.* **2006**, *33*, L22812.

28.   Hains, J. C.; Taubman, B. F.; Thompson, A. M.; Marufu, L. T.; Stehr, J. W.; Dickerson, R. R. Origins of Chemical Pollution Derived from Mid-Atlantic Aircraft Profiles Using a Clustering Technique. *J. Geophys. Res.* **2008**, *42* (8), 1727-1741.

29.   Bloomer, B. J. Air Pollution Response to Emissions Changes at Power Plants in the Eastern United States. Ph.D. Thesis, University of Maryland, College Park, MD, 2008.

30.   Berman, S.; Ku, J. Y.; Rao, S. T. Spatial and Temporal Variation in the Mixing Depth over the Northeastern United States during the Summer of 1995. *J. Appl. Meteor.* **1999**, *38* (12), 1661-1673.

31.   Rao, S. T.; Ku, J. Y.; Berman, S.; Zhang, K.; Mao, H. Summertime Characteristics of the Atmospheric Boundary Layer and Relationships to Ozone Levels over the Eastern United States. *Pure Appl. Geophys.* **2003**, *160*, 21-55.

32.   Faraji, M.; Kimura, Y.; McDonald-Buller, E.; Allen, D. Comparison of the carbon bond and SAPRC photochemical mechanisms under conditions relevant to southeast Texas. *Atmos. Environ.* **2008**, *42*, 5821-5836.